THE JOURNAL OF PHYSICAL CHEMISTRY Letters

LETTER

pubs.acs.org/JPCL

Utilization of Direct and Diffuse Sunlight in a Dye-Sensitized Solar Cell — Silicon Photovoltaic Hybrid Concentrator System

Greg D. Barber,[*,†] Paul G. Hoertz,[†] Seung-Hyun Anna Lee,[†] Neal M. Abrams,[†] Janine Mikulca,[†] Thomas E. Mallouk,[†] Paul Liska,[‡] Shaik M. Zakeeruddin,[‡] Michael Grätzel,[‡] Anita Ho-Baillie,[§] and Martin A. Green[§]

[†]Department of Chemistry and Materials Research Institute, The Pennsylvania State University, University Park, Pennsylvania 16801, United States

[‡]Laboratory of Photonics and Interfaces, École Polytechnique Fédérale de Lausanne, Lausanne, Switzerland

[§]ARC Photovoltaics Centre of Excellence, School of Photovoltaic and Renewable Energy Engineering, University of New South Wales, Sydney, Australia

S Supporting Information

ABSTRACT: The concept of a tandem hybrid concentrator solar module was demonstrated from a dye-sensitized TiO_2 solar cell (DSSCs) and a silicon p−n junction solar cell. The test system employed DSSC and Si cells with indoor AM1.5G efficiencies of 9.1 and 18.1%, respectively. Two different optical filters were used to selectively reflect and concentrate near-infrared light from the DSSC onto the Si cell. On the basis of outdoor testing in a 2× concentrator−reflector arrangement, the tandem system generated 93 and 96% of the output power of directly illuminated Si cells under altostratus/cirrostratus and clear sky irradiances, respectively, despite a DSSC-to-Si active area ratio of only 0.92. Similar performance is expected at higher (5−10×) concentration ratios. The hybrid arrangement of visible- and IR-absorbing solar cells addresses the problem of lower performance of conventional concentrators under diffuse irradiance conditions. These proof-of-concept results suggest that system level efficiencies approaching 20% should be achievable.

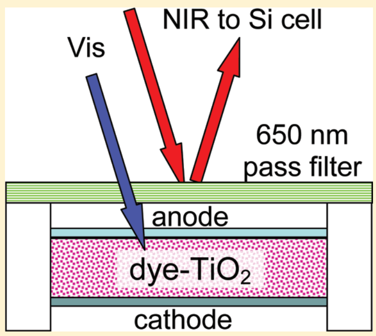

SECTION: Energy Conversion and Storage

Because solar energy is a ubiquitous but low-energy density resource, there is a need for low-cost photovoltaic systems that work efficiently under a range of irradiation conditions. Solar photovoltaic technology is currently dominated by solid-state single-junction flat plate systems in which silicon is the most common active solar absorber material. Conventional silicon modules are up to 13% efficient,[1] with costs proportional to efficiency and area. The recent commercialization of HIT Si cells has increased module efficiency to over 20% but with a corresponding increase in cost. With flat plate solar cells, the active solar material is the major cost component, and the abundance of elements such as In (in $CuIn_{1-x}Ga_xSe_2$, CIGS) and Te (in CdTe) as well as Si refining supply market demand shortages[2] create problems of scalability.

Solar concentrator systems can, in principle, minimize the impact of the cost and abundance of active semiconductor materials. The highest-efficiency photovoltaic concentrator systems use multijunction III−V cells similar to those developed for the space program. These cells can have laboratory efficiencies in excess of 39%[3] under the reference concentrator solar spectrum, which is reduced by 10−23% when referenced to the global solar spectrum.[4] At typical concentration ratios of 250−1000 suns,[5] these cells require precise tracking and dissipate thermal loads that are comparable to today's most highly developed microprocessors (10s W/cm^2).

A drawback of concentrator systems, whether single- (e.g., Si) or multijunction (III−V), is that they do not effectively use the diffuse component of solar radiation. They are thus generally deployed in geographical regions of high direct normal sunlight. Even under a cloudless sky, the consequences of atmospheric scattering are evident by comparing the direct normal and global (direct normal plus diffuse) radiation reference spectra shown in Figure 1.[6] The global radiation reference spectrum has significantly more power in the visible because of the wavelength dependence of scattering. As scattering increases, for example because of intermittent or thin cloud layers, a greater proportion of direct radiation in the visible becomes diffuse, and a concentrator's output power diminishes. This variability in direct and diffuse radiation is a reason why flat plate solar products are so widely used.

Nanocrystalline dye-sensitized solar cells (DSSCs) and organic photovoltaics (OPV) are two families of low-cost solar devices that absorb light in the visible part of the spectrum.[7] While several factors contribute to energy losses and the "low" efficiencies of these cells, a very important one is their poor response to red and near-infrared light. This is illustrated in Figure 2, which shows the absorbance spectrum of a typical DSSC sensitized with the most widely studied N719 dye.[8] Because the spectral region in which these DSSCs absorb comprises only about 40% of the energy of the solar spectrum, it follows that the efficiency of DSSCs in the visible (400−650

Received: January 24, 2011
Accepted: February 10, 2011

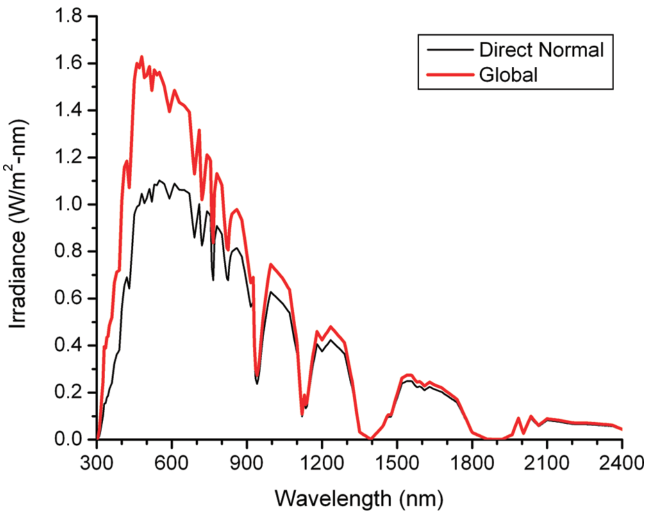

Figure 1. Reference direct normal (black) and global (direct normal plus diffuse, red) terrestrial solar power spectra. The direct normal spectrum is attenuated, primarily in the visible part of the spectrum, by atmospheric scattering.

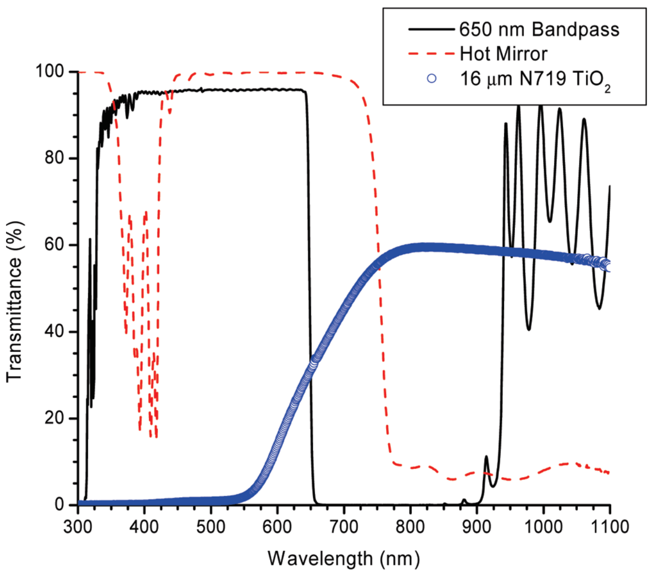

Figure 2. Transmission spectra of band-pass (solid line) and hot mirror (red dashed line) filters used for indoor and outdoor testing of DSSCs and Si concentrator cells along with the transmission spectrum of a typical 16 μm thick titania (TiO_2) DSSC anode sensitized with the most widely studied N719 dye.

nm) is over two times the full spectrum value. Thus, 10% efficient DSSCs can be >20% efficient solar cells in their useful spectral range. Figure 2 also shows the reflectance spectra of band-pass and hot mirror filters,[9] which transmit light in the part of the spectrum absorbed by the DSSC and efficiently reflect light in the part of the spectrum most efficiently used by Si cells.

Because the red and near-infrared parts of the solar spectrum are not utilized efficiently by dye (or OPV) cells, a number of approaches including panchromatic dye molecules,[10,11] light scattering by photonic crystal layers,[12−19] integration of optical fibers,[20] bifacial cells,[21] and combinations of multiple absorbers[22,23] have been investigated to improve their spectral response. So far, none of these has yielded efficiencies beyond that realized in the best conventional DSSCs. Another approach is to construct tandem cells in which DSSC and narrow-band-gap (e.g., Si or CIGS) cells are stacked in series.[24−27] While efficiencies up to 15% have been reported,[24] the tandem arrangement requires equal areas of the solid state and dye cell (adding to cost), and it incurs the infrared transmission losses of the transparent conducting oxide.

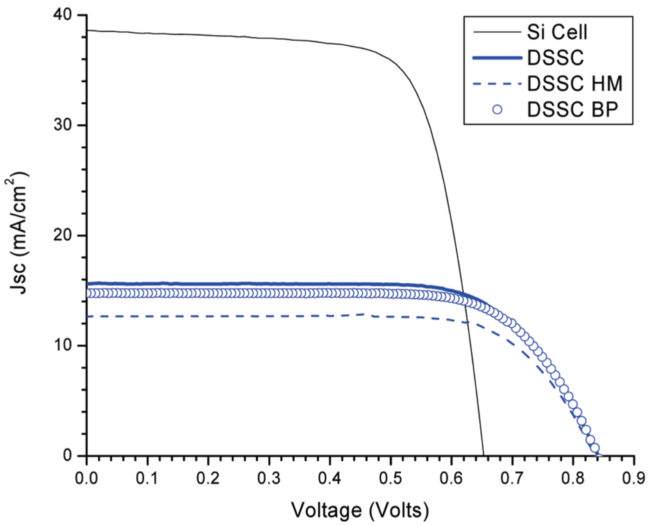

Figure 3. Current−voltage curves for DSSC and Si cells with collimated AM1.5 radiation at 100 mW/cm^2. Dashed and dotted curves show the performance of the DSSC when coupled to a hot mirror (DSSC HM) or 650 nm band-pass filter (DSSC BP).

An alternative design, which is described here, uses a DSSC with a short-band-pass filter to selectively reflect and concentrate near-IR light to a Si cell. This arrangement allows the DSSC to utilize both direct and diffusely scattered visible light while directing the low-scattering near-IR light onto the more efficient Si cell. The cost of the latter component is minimized by light concentration. An additional benefit of this arrangement at low (5−10×) concentration ratios is that the silicon cell should maintain its efficiency because of the increase in open-circuit voltage with photon flux[28] and the lower thermalization per electron relative to full-spectrum concentrators. Although spectrum-splitting schemes have been considered for Cassegrian concentrators and related designs, such systems focus light using reflective or refractive optics onto both the narrow and wide-band-gap absorbers, and thus, they do not efficiently utilize the diffuse component of solar radiation.[29−31] Recently, Rühle et al. have demonstrated spectrum splitting using dichroic mirrors in a DSSC-GaInP photovoltaic device.[32] While they did not explore the idea of light concentration to minimize the area of the expensive infrared-absorbing cells, they did show substantially enhanced solar performance relative to either component alone.

Figure 3 shows the results of indoor testing of the DSSC and Si p−n junction cells, and performance data are summarized in Table 1. A collimated Xe lamp source, filtered to simulate the AM1.5 global spectral irradiance, provides only direct normal radiation with essentially no diffuse component. As expected, the power curves show higher photocurrent density for the Si cell, which utilizes almost the entire solar power spectrum and lower photocurrent but higher photovoltage for the visible-light-absorbing DSSC. Under full spectrum conditions, the efficiencies of the DSSC and Si cells are 9.1 and 18.1%, respectively. The dashed

dx.doi.org/10.1021/jz200112m |J. Phys. Chem. Lett. 2011, 2, 581–585

Table 1. Indoor Solar Performance of the Silicon ($0.94\ cm^2$) and DSSC ($0.865\ cm^2$) in This Work under the AM1.5G Class A Solar Simulator[a]

cell, active area, and filter	V_{oc} (V)	I_{sc} (mA)	J_{sc} (mA/cm^2)	FF (%)	power max (mW)	efficiency (%)
Si cell, no filter, 100 mW/cm^2	0.651	36.250	38.56	72.1	17.01	18.10
DSSC, no filter, 100 mW/cm^2	0.841	13.481	15.58	69.64	7.90	9.13
DSSC with 650 nm band-pass (total incident 100 mW/cm^2)	0.843	12.738	14.73	70.73	7.59	8.77
DSSC with 650 nm filter calculated using transmitted power of 65 mW/cm^2						13.50
DSSC with hot mirror (total incident 100 mW/cm^2)	0.834	10.501	12.14	72.42	6.34	7.33
DSSC with hot mirror calculated using transmitted power of 38 mW/cm^2						19.29

[a] The DSSC was also measured with two short-pass filters to show the variation in efficiency with selective bands of solar radiation despite having lower maximum power points than those under full AM1.5G conditions.

Scheme 1. Hybrid Concentrator Arrangement Used in Outdoor Testing

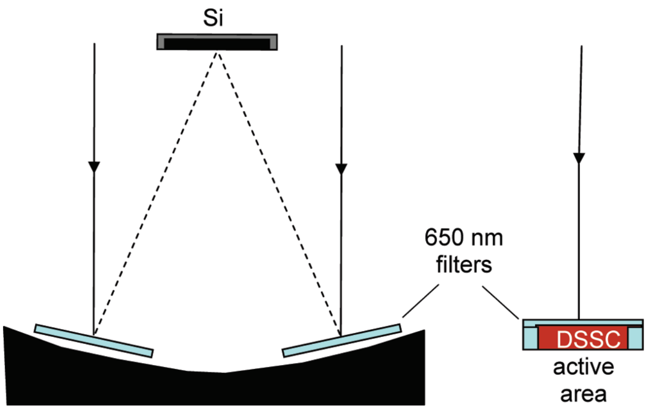

lines show power curves for the same DSSC with a hot mirror or band-pass filter coupled to its illuminated anode face. Because the hot mirror reflects some of the light in the 360−450 nm range, there is a 22% drop in short-circuit photocurrent relative to the unfiltered DSSC. However, the efficiency of the DSSC, calculated on the basis of transmitted power, increases to 19.3%. In the case of the band-pass filter, the photocurrent of the DSSC drops by only 6% because under full-spectrum irradiation, it does not use wavelengths longer than 650 nm. The efficiency based on transmitted light increases to 13.5%. This increase in efficiency is not as dramatic as that with the hot mirror filter because of the higher transmittance of the band-pass filter to infrared radiation past 900 nm, as shown in Figure 2.

Because the 650 nm band-pass/DSSC arrangement gave higher photocurrent, this combination was used in subsequent outdoor testing on two days that provided clear and altostratus/cirrostratus conditions, where the average diffuse component of the global power was 9.8 and 14.5%, respectively. On each test day, DSSC power curves were obtained with and without the 650 nm band-pass filter, and Si power curves were measured in full sun. Next, two band-pass filters were used to reflect the red−infrared part of the incident light onto the Si cell, as shown in the reflector−2× concentrator arrangement sketched in Scheme 1. The results are summarized in Table 2, where duplicate entries illustrate the performance variation at different times during the measurement period.

The simplest way to interpret the data shown in Table 2 is to calculate the power generated by a hybrid concentrator consisting of two DSSCs with 650 nm filters reflecting light to one Si cell and to compare it to the power of two directly illuminated Si cells under global irradiance. This comparison is not made under optimum area ratio conditions for the concentrator because the active area of the DSSC was only 92% of the active area of the Si cell. Nevertheless, it gives an idea of the power of a 2× concentrator (which uses half of the number of Si cells) relative to a flat plate Si module of the same area as the DSSCs. Under clear sky conditions, the hybrid concentrator generates $16.98 + 2 \times 6.91 = 30.80$ mW, which is 96.5% of the power (31.91 mW) of two Si cells under global irradiance (i.e., without mirrors). Under altostratus/cirrostratus conditions, the concentrator system generated 26.67 mW, which is 93.1% of the power (27.86 mW) of the two Si cells. The very modest decrease in going from clear to scattering conditions can be understood by referring to Figures 1 and 2. Very little of the scattered light is in the part of the spectrum that is reflected to the Si cell. The experiment under altostratus/cirrostratus conditions in particular demonstrates the improvement in module efficiency relative to a conventional parabolic mirror concentrator. In addition to reflectance losses from the mirrors, a conventional concentrator would be expected to lose essentially all of the diffuse power (here 14.5%) in the global spectrum.

While the hybrid concentrator system described here was designed for proof-of-concept purposes, several important features in the design of practical modules are noted. First, the area concentration ratio can likely be increased to 5−10× without active cooling of the Si cell. Preliminary data show that the performance of the Si cell remains essentially constant up to 7× because the increased photovoltage from higher flux compensates the loss from heating. At 5−10× concentration, the cost of the Si cell relative to other components of the system is dramatically reduced. Second, higher-performing DSSC and Si cells have been reported, and the band-pass filter is not perfectly matched to the DSSC absorbance spectrum. With higher-performing DSSCs[8,33−37] and better spectral matching of filters, the efficiency of the module (here 16.3 and 19.1% under alto/cirrostratus and clear sky conditions on an active area basis) could exceed 20%. Third, Si could also be replaced by another efficient flat plate absorber such as CIGS because they operate over the same spectral range. The DSSC could be replaced by OPV, thin-film CdTe, or II−VI quantum dot cells, which absorb primarily in the visible. Thus, the hybrid concentrator arrangement provides a new way to incorporate inexpensive, chemically processed solar cell materials into efficient modules. Finally, it may be possible to design systems based on refractive optics[37] that selectively concentrate infrared light to small Si cells at their focus and transmit or scatter visible light to a larger visible-absorbing back plane. Miniaturization of the Si cells and lenses

Table 2. Outdoor Solar Performance Characteristics of the DSSC and Si Cell under Global Irradiance and with a 650 nm Short-Band-Pass (BP) Filter

	V_{oc} (V)	I_{sc} (mA)	J_{sc} (mA/cm^2)	FF	power (mW)	active area efficiency
Altostratus/Cirrostratus (Average Global: 88.3 mW/cm^2)						
Si global irradiance	0.618	29.85	31.76	0.755	13.93	16.78
Si with two filter reflectors	0.613	28.13	29.93	0.743	12.81	15.44
	0.614	29.44	31.32	0.753	13.61	16.40
DSSC global irradiance	0.835	11.27	13.03	0.716	6.74	8.82
	0.832	10.30	11.90	0.746	6.39	8.36
DSSC 650 nm BP filter	0.836	10.19	11.78	0.733	6.24	8.18
	0.836	10.93	12.63	0.711	6.50	8.50
Clear Sky Testing (Average Global: 89.1 mW/cm^2)						
Si global irradiance	0.647	34.34	36.53	0.745	16.55	19.76
	0.638	34.19	36.37	0.704	15.36	18.34
Si with two filter reflectors	0.64	35.73	38.01	0.742	16.98	20.26
DSSC global irradiance	0.824	12.91	14.92	0.704	7.49	9.71
DSSC 650 nm BP filter	0.821	12.11	14.01	0.695	6.91	8.97

would decrease the vertical dimensions of these systems and potentially eliminate the need for two-axis tracking. Clever techniques for fabricating concentrator microcell arrays have recently been described.[38] Ultimately, it may be possible to create stationary modules with the form factor of flat panel systems that combine an inexpensive large-area visible absorber with small amounts of Si to achieve high efficiency. These ideas are currently being explored experimentally.

ASSOCIATED CONTENT

S Supporting Information. Experimental details of cell preparation and testing. This material is available free of charge via the Internet at http://pubs.acs.org.

AUTHOR INFORMATION

Corresponding Author
*E-mail: gdb102@psu.edu.

ACKNOWLEDGMENT

This work was supported by the U.S. Department of Energy, Office of Basic Energy Sciences, under Contracts DE-FG02-05ER15756 and DE-FG02-07ER15911. P.L., S.M.Z., and M.G. acknowledge financial support of this work by EU project "ROBUST DSC" Grant Agreement Number 212792. The authors thank Nathan Neale, Arthur Frank, and Toby Meyer for helpful advice and discussions. We thank Ferro Corporation and Nippon Sheet Glass for providing samples of materials and Kent Terwilliger, Elizabeth Mack, Jonathan Perez-Blanco, Bradley Lewis, Amanda Jane Lind, and James Broyles for experimental support.

REFERENCES

(1) del Cueto, J. A. Comparison of Energy Production and Performance from Flat-Plate Photovoltaic Module Technologies Deployed at Fixed Tilt. *Publication NREL/CP-520-31444*; U.S. Department of Commerce, National Technical Information Service: Springfield, VA, May 2002.

(2) Buonassisi, T.; Istratov, A. A.; Marcus, M. A.; Lai, B.; Cai, Z.; Heald, S. M.; Weber, E. R. Engineering Metal-Impurity Nanodefects For Low-Cost Solar Cells. *Nat. Mater.* **2005**, *4*, 676–679.

(3) Dimroth, F. High-Efficiency Solar Cells From III-V Compound Semiconductors. *Phys. Status Solidi C* **2006**, *3*, 373–379.

(4) Myers, D. R.; Emery, K. E.; Gueymard, C. Proposed Reference Spectral Irradiance Standards to Improve Concentrating Photovoltaic System Design and Performance Evaluation. *Publication NREL/CP-520-31406*; U.S. Department of Commerce, National Technical Information Service: Springfield, May 2002.

(5) Ward, J.; Ramanathan, K.; Hasoon, F.; Coutts, T.; Keane, J.; Moriarty, T.; Noufi, R. Cu(In,Ga)Se_2 Thin Film Concentrator Solar Cells. *Publication NREL/CP-520-31144*; U.S. Department of Commerce, National Technical Information Service: Springfield, October 2001.

(6) American Society for Testing of Materials (ASTM) standard E891 Tables for Terrestrial Direct Normal Solar Spectral Irradiance Tables for Air Mass 1.5 and standard E892 Tables for Terrestrial Solar Spectral Irradiance at Air Mass 1.5 for a 37-Deg Tilted Surface were withdrawn in 1999 and replaced by standard G159-98, which was withdrawn in 2005 and replaced by G173-03e1 Standard Tables for Reference Solar Spectral Irradiances: Direct Normal and Hemispherical on 37° Tilted Surface. The data tables represent reasonable cloudless atmospheric conditions favorable for photovoltaic (PV) energy production, as well as weathering and durability exposure applications. (ASTM International, 2005).

(7) Grätzel, M. Photoelectrochemical Cells. *Nature* **2001**, *414*, 338–344.

(8) Nazeeruddin, M. K.; Kay, A.; Rodicio, I.; Humphry-Baker, R.; Mueller, E.; Liska, P.; Vlachopoulos, N.; Grätzel, M. Conversion of Light to Electricity by Cis-X2bis(2,2′-bipyridyl-4,4′-dicarboxylate)ruthenium(II) Charge-Transfer Sensitizers (X = Cl-, Br-, I-, CN-, and SCN-) on Nanocrystalline Titanium Dioxide Electrodes. *J. Am. Chem. Soc.* **1993**, *115*, 6382–6390.

(9) Freeman, M. H. *Optics*, 10th ed.; Butterworths: Markham, ON, Canada, 1990; pp 418−419.

(10) Nazeeruddin, M. K.; Péchy, P.; Renouard, T.; Zakeeruddin, S. M.; Humphrey-Baker, R.; Comte, P.; Liska, P.; Le Cevey, E. C.; Shklover, V.; Spiccia, L.; Deacon, G. B.; Bignozzi, C. A.; Grätzel, M. Engineering of Efficient Panchromatic Sensitizers for Nanocrytalline TiO_2-Based Solar Cells. *J. Am. Chem. Soc.* **2001**, *123*, 1613–1624.

(11) Miyasaka, T. Toward Printable Sensitized Mesoscopic Solar Cells: Light-Harvesting Management with Thin TiO_2 Films. *J. Phys. Chem. Lett.* **2011**, *2*, 262–269.

(12) Nishimura, S.; Abrams, N.; Lewis, B. A.; Halaoui, L. I.; Mallouk, T. E.; Benkstein, K. D.; van de Lagemaat, J.; Frank, A. Standing Wave

Enhancement of Red Absorbance and Photocurrent in Dye-Sensitized Titanium Dioxide Photoelectrodes Coupled to Photonic Crystals. *J. Am. Chem. Soc.* **2003**, *125*, 6306–6310.

(13) Mihi, A.; Miguez, H. Origin of Light-Harvesting Enhancement in Colloidal-Photonic-Crystal-Based Dye-Sensitized Solar Cells. *J. Phys. Chem. B* **2005**, *109*, 15968–15976.

(14) Halaoui, L.; Abrams, N.; Mallouk, T. E. Increasing the Conversion Efficiency of Dye-Sensitized TiO_2 Photoelectrochemical Cells by Coupling to Photonic Crystals. *J. Phys. Chem. B* **2005**, *109*, 6334–6342.

(15) Mihi, A.; Calvo, M. E.; Anta, J. A.; Miguez, H. Spectral Response of Opal-Based Dye-Sensitized Solar Cells. *J. Phys. Chem. C* **2008**, *112*, 13–17.

(16) Colodrero, S.; Mihi, A.; Haggman, L.; Ocana, M.; Boschloo, G.; Hagfeldt, A.; Miguez, H. Porous One-Dimensional Photonic Crystals Improve the Power-Conversion Efficiency of Dye-Sensitized Solar Cells. *Adv. Mater.* **2009**, *21*, 764.

(17) Lee, S.-H. A.; Abrams, N. M.; Hoertz, P. G.; Barber, G. D.; Halaoui, L. I.; Mallouk, T. E. Coupling of Titania Inverse Opals to Nanocrystalline Titania Layers in Dye-Sensitized Solar Cells. *J. Phys. Chem. B* **2008**, *112*, 14415–14421.

(18) Guldin, S.; Hüttner, S.; Kolle, M.; Welland, M. E.; Müller-Buschbaum, P.; Friend, R. H.; Steiner, Y.; Tétreault, N. Dye-Sensitized Solar Cell Based on a Three-Dimensional Photonic Crystal. *Nano Lett.* **2010**, *10*, 2303–2309.

(19) Shin, J.-H.; Kang, J.-H.; Jin, W.-M.; Park, J. H.; Cho, Y.-S.; Moon, H. Facile Synthesis of TiO_2 Inverse Opal Electrodes for Dye-Sensitized Solar Cells. *Langmuir* **2011**, *27*, 856–860.

(20) Weintraub, B.; Wei, Y.; Wang, Z. L. Optical Fiber/Nanowire Hybrid Structures for Efficient Three-Dimensional Dye-Sensitized Solar Cells. *Angew. Chem., Int. Ed.* **2009**, *48*, 8981–8985.

(21) Ito, S.; Zakeeruddin, S. M.; Comte, P.; Liska, P.; Kuang, D.; Graetzel, M. *Nat. Photonics* **2008**, *2*, 693–698.

(22) Basham., J. I.; Mor, G. K.; Grimes, C. A. Förster Resonance Energy Transfer in Dye-Sensitized Solar Cells. *ACS Nano* **2010**, *4*, 1253–1258.

(23) Shalom, M.; Albero, J.; Tachan, Z.; Martinez-Ferrero, E.; Zaban, A.; Palomares, E. Quantum Dot—Dye Bilayer-Sensitized Solar Cells: Breaking the Limits Imposed by the Low Absorbance of Dye Monolayers. *J. Phys. Chem. Lett.* **2010**, *1*, 1134–1138.

(24) Liska, P.; Thampi, K. R.; Grätzel, M.; Bremaud, D.; Rudmann, D.; Upadhyaya, H. M.; Tiwari, A. N. Nanocrystalline Dye-Sensitized Solar Cell/Copper Indium Gallium Selenide Thin-Film Tandem Showing Greater than 15% Conversion Efficiency. *Appl. Phys. Lett.* **2006**, *88*, 203103–203103/3.

(25) Durr, M.; Bamedi, A.; Yasuda, A.; Nelles, G. Tandem Dye-Sensitized Solar Cell For Improved Power Conversion Efficiencies. *Appl. Phys. Lett.* **2004**, *84*, 3397–3399.

(26) Usagawa, J.; Pandey, S. S.; Hayase, S.; Kono, M.; Yamaguchi, Y. Tandem Dye-Sensitized Solar Cells Fabricated on Glass Rod without Transparent Conductive Layers. *Appl. Phys. Express* **2009**, *2*, 062203.

(27) Guo, X.-Z.; Zhang, Y.-D.; Qin, D.; Luo, Y.-H.; Li, D.-M.; Pang, Y.-T.; Meng, Q.-B. Hybrid Tandem Solar Cell for Concurrently Converting Light and Heat Energy with Utilization of Full Solar Spectrum. *J. Power Sources* **2010**, *195*, 7684–7690.

(28) Green., M. A., Holonyak, N., Jr., Eds. *Solar Cells: Operating Principles, Technology, and System Applications*; Prentice Hall: New York, 1982; Chapter 4.

(29) Lewis M. Fraas, L. M.; Avery, J. E.; Huang, H. X., Shifman, E.; Edmondson, K.; King, R. R. Toward 40% and Higher Multijunction Cells in a New Cassegrain PV Module. 31stst IEEE PVSC, Florida, U.S. A., Jan. 2005; pp 751—753.

(30) Imenes, A. G.; Buie, D.; Mills, D. R.; Schramek, P.; Bosi, S. G. A New Strategy For Improved Spectral Performance In Solar Power Plants. *Solar Energy* **2008**, *80*, 1263–1269.

(31) Goetzberger, A.; Goldschmidt, J. C.; Peters, M.; Löper, P. Light Trapping, A New Approach to Spectrum Splitting. *Solar Energy Mater. Solar Cells* **2008**, *92*, 1570–1578.

(32) Rühle, S.; Segai, A.; Vilan, A.; Kurtz, S. R.; Grinis, L.; Zaban, A.; Lubomirsky, I.; Cahen, D. A Two Junction, Four Terminal Photovoltaic Device for Enhanced Light to Electric Power Conversion Using a Low-Cost Dichroic Mirror. *J. Renewable Sustainable Energy* **2009**, *1*, 013106.

(33) Wang, Z.-S.; Kawauchi, H.; Kashima, T.; Arakawa, H. Significant Influence of TiO_2 Photoelectrode Morphology on the Energy Conversion Efficiency of N719 Dye-Sensitized Solar Cell. *Coord. Chem. Rev.* **2004**, *248*, 1381–1389.

(34) Meyer, T. B.; Azam, A.; Meyer, A. F. First Large-Area Dye Solar Cells. *Proc. SPIE* **2004**, *5215*, 1–8.

(35) Toyoda, T.; Sano, T.; Nakajima, J; Doi, S.; Fukumoto, S.; Ito, A.; Tohyama, T.; et al. Outdoor Performance of Large Scale DSC Modules. *J. Photochem. Photobiol., A* **2004**, *164*, 203–207.

(36) Kroon, J. M.; Bakker, N. J.; Smit, H. J. P.; Liska, P.; Thampi, K. R.; Wang, P.; Zakeeruddin, S. M.; Grätzel, M.; Hinsch, A.; Hore, S.; Würfel, U.; Sastrawan, R.; Durrant, J. R.; Palomares, E.; Pettersson, H.; Gruszecki, T.; Walter, J.; Skupien, K.; Tulloch, G. E. Nanocrystalline Dye-Sensitized Solar Cells Having Maximum Performance. *Progr. Photovoltaics Res. Appl.* **2007**, *15*, 1–18.

(37) Green, M. A., Kamiya, T., Monemar, B., Venghaus, H., Yamamoto, Y., Eds. *Third Generation Photovoltaics, Advanced Solar Energy Conversion*; Springer: New York, 2003; Chapter 2.

(38) Yoon, J.; Baca, A. J.; Park, S.-I.; Elvikis, P.; Geddes, J. B.; Li, L.; Kim, R. H.; Xiao, J.; Wang, S.; Kim, T. H.; Motala, M. J.; Ahn, B. Y.; Duoss, E. B.; Lewis, J. A.; Nuzzo, R. G.; Ferreira, P. M.; Huang, Y.; Rockett, A.; Rogers, J. A. Ultrathin Silicon Solar Microcells for Semitransparent, Mechanically Flexible and Microconcentrator Module Designs. *Nat. Mater.* **2008**, *7*, 907–915.